International Journal of Mechanical Sciences 135 (2018) 226–239

Contents lists available at ScienceDirect

International Journal of Mechanical Sciences

journal homepage: www.elsevier.com/locate/ijmecsci

Damage evolution and ductile fracture prediction during tube spinning of titanium alloy

Wenchen Xu*, He Wu, Hao Ma, Debin Shan*

School of Materials Science and Engineering & National Key Laboratory for Precision Hot Processing of Metals, Harbin Institute of Technology, Harbin 150001, PR China

ARTICLE INFO

Keywords:
Ductile fracture criteria
Damage
Tube spinning
Damage limit

ABSTRACT

In order to analyze and control surface crack during tube spinning of titanium alloy, six ductile fracture criteria (DFCs) were incorporated into the finite element software (ABAQUS) to simulate the damage evolution in the tube spinning process under various thinning rates. For improving the prediction accuracy of damage evolution during tube spinning, the valid damage strain was proposed to eliminate or diminish the strain fluctuation caused by the ALE adaptive meshing technique. Through analyzing the influence of the equivalent plastic strain, stress state and the principal stresses on the damage accumulation, the mechanisms of surface cracks were revealed. The results show that only the McClintock model predicted that the crack in tube spinning of Ti–15–3 alloy could be eliminated under moderate thinning rates, while lower or higher thinning rates may induce cracking on the tube surface, which was consistent with the experimental results. For the outer layer, as the thinning rate increased, the increasing equivalent plastic strain and tensile principal stresses contributed to the damage accumulation for all the DFCs studied in present research. For the inner layer under moderate thinning rates, the compressive axial and tangential stresses slowed down the damage accumulation, leading to the occurrence of the safe zone of thinning rate (~20–30%) without surface crack during tube spinning of Ti–15–3 alloy.

1. Introduction

Tube spinning is an advanced forming process to produce thin-walled tubular workpieces with high precision and improved mechanical properties, widely used in aviation, chemistry, power industries, etc. [1,2]. During tube spinning, a tubular-shaped metal blank or workpiece placed over a mandrel is shaped via radial compressive forces applied by the rollers. In this way, the wall thickness is reduced as the material is encouraged to flow mainly in the axial direction of the mandrel, increasing the length of the workpiece. Due to high precision and productivity as well as low cost, cold spinning is preferred in spinning practice. However, it is quite hard to manufacture tubular components of difficult-to-deform metal materials, such as titanium alloys, through the cold spinning process due to their low ductility and high work hardening rate at room temperature [3]. In tube spinning of titanium alloy, surface cracking often takes place in as-spun workpieces [4,5]. Usually, cracking is caused by severe plastic deformation which exceeds the material forming limit. For the tube spinning process, low material ductility and great thinning rates of wall thickness could induce spinning crack. Nevertheless, the cracks are also prone to emerge at smaller thickness reduction, even under heating condition, while vanish at moderate thinning rates in tube spinning of low-ductility metals [4,6], indicating the complexity of formation of spinning crack. Hence, it is necessary to reveal the mechanism of spinning crack for low-ductility materials and propose effective measures to prevent spinning cracking, which is the prerequisite for the realization of cold spinning of titanium alloys.

In order to find proper processing conditions for each material, the forming limit, i.e. the fracture initiation in forming process should be predicted correctly. In case of titanium alloys with low ductility, ductile fracture with slight necking cannot be estimated reasonably by conventional forming limit diagrams (FLDs) and other necking-based models [7-9]. Instead of common necking models, ductile fracture criteria (DFCs) have attracted increasing attentions to assess the initiation of deformation failure in metal forming processes, such as shear and compression with low and negative stress triaxiality. The coupling of DFCs with finite element (FE) simulation was more and more used to predict crack initiation, propagation, and final rupture during metal forming [8,10-13]. Nevertheless, the applications of DFCs are still limited in the spinning process. The Gurson–Tvergaard–Needleman (GTN) model has been employed to study the damage evolution in the spinning process by some researchers. Li et al. [14] and Wang et al. [15] suggested that the GTN model was inappropriate for spinning process due to low stress triaxialities. Besides, Zhan et al. [16] performed the damage simulation of shear spinning using the Lemaitre model. However, the CDM-based ductile fracture model did not consider plastic deformation localization,

* Corresponding authors.
E-mail address: xuwc_76@hit.edu.cn (W. Xu).

https://doi.org/10.1016/j.ijmecsci.2017.11.024
Received 12 July 2017; Received in revised form 29 October 2017; Accepted 15 November 2017
Available online 15 November 2017
0020-7403/

easily leading to incorrect prediction of damage evolution under complex deformation conditions [17]. Ma et al. [18] simulated and analyzed the damage evolution in the tube spinnability test, and compared the prediction accuracy of various DFCs on the fracture limit beyond which spinning crack would take place. However, the fracture location and mechanism of the surface crack during tube spinning of low-ductility materials under various thinning rates has not been reported clearly until now.

In this study, the tube spinning process was modeled by three-dimensional finite element method (FEM) and the spinning experiments of Ti–15–3 alloy were conducted under different thinning rates. Six ductile fracture criteria were incorporated into the finite element software (ABAQUS) to simulate the damage evolution in the tube spinning process. To reveal the mechanism of surface crack, the vital factors, such as the equivalent plastic strain, stress state and the principal stresses, which influenced the damage accumulation were analyzed. Furthermore, the propagation of ductile crack under different thinning rates was discussed and compared.

2. Development of ductile fracture criteria (DFCs)

At the microscopic level, microvoid nucleation, growth and coalescence, has been regarded as one of the most important mechanism of ductile failure of metallic materials. On this basis, a number of mathematical models have been proposed to describe the ductile fracture behavior. Currently, all the ductile fracture criteria can be classified into two categories for fracture prediction. The first category, i.e. coupled ductile fracture criterion (DFC), introduces damage variable into material constitutive relationships. One of the most popular coupled ductile fracture criteria is the Gurson fracture model, which extends the von Mises plasticity model to porous materials, whose behavior depends on first stress invariant and is based on cell calculations [19], while they are not appropriate for low stress triaxialities [14,20]. Hence, an alternative type of the coupled models has been proposed to treat damage evolution in a macroscopic and phenomenological way. Under the framework of continuum damage mechanics (CDM), Lemaitre [21] developed the phenomenological damage models by defining the damage process as an irreversible process. However, the CDM-based ductile fracture model does not consider plastic deformation localization, easily leading to inappropriate prediction of damage evolution under some deformation conditions, such as uniaxial tension [17].

The other category, i.e. uncoupled ductile fracture criteria, neglects the influence of damage on the material constitutive relationships and describes the critical loading condition by a weighted function of equivalent plastic strain depending on the stress states. In comparison to the complicated coupled DFCs, the uncoupled models have been more extensively utilized for industry application because of their inherent simplicity and less parameters needed to be evaluated through experimental data. Based on the energy principle, the earlier uncoupled DFC was proposed by Freudenthal [22], in which ductile fracture was mainly dominated by the plastic work. Cockcroft and Latham [23] developed an empirical energetic damage criterion, who indicated that the fracture often occurred in the maximum principal tensile stress zone. Further, Oh et al. [24] put forward a normalized Cockcroft–Latham criterion to promote the prediction accuracy in the extrusion and drawing process. Brozzo et al. [25] improved the prediction of formability limits of metal sheets by empirically coupling the effect of hydrostatic stress into the C–L criterion. McClintock [26] proposed a ductile fracture criterion based on the analytical expansion of growth of cylindrical under the axes of the cylindrical parallel to the principal stress axes. Based on Drucker's stability postulate, Rice and Tracey [27] introduced a function to describe the void growth by an exponential function of stress triaxiality, which was also adopted in the Ayada et al. [28] ductile fracture criterion. Ma et al. [18] coupled the critical value of −1/3 into the Ayada model, enlarging the applicability of Ayada model. Also, LeRoy et al. [29] modified the Rice and Tracey model by analyzing the evolution of nucleation, shape change and coalescence of voids. Our previous research on the damage evolution in the tube spinnability test indicates that all the ductile fracture criteria above mentioned correctly predicted the damage distribution on TA2 titanium tubes in the tube spinnability tests except for the Freudenthal, Rice-Tracey and Ayada models [18]. Therefore, we primarily considered the remaining uncoupled DFCs in tube spinning process in the present study, as listed in Table 1.

Table 1
Brief summary of selected typical uncoupled DFCs.

Criterion	Formula
Cockcroft and Latham (C–L)	$\int_0^{\bar{\varepsilon}_f^p} \sigma_1 d\bar{\varepsilon}^p = c_1$
Oh et al. (Oh)	$\int_0^{\bar{\varepsilon}_f^p} \frac{\sigma_1}{\bar{\sigma}} d\bar{\varepsilon}^p = c_2$
Brozzo et al. (Brozzo)	$\int_0^{\bar{\varepsilon}_f^p} \frac{2\sigma_1}{3(\sigma_1-\sigma_m)} d\bar{\varepsilon}^p = c_3$
McClintock	$\int_0^{\bar{\varepsilon}_f^p} [\frac{\sqrt{3}}{2(1-n)} \sinh\{\frac{\sqrt{3}}{2(1-n)} \frac{\sigma_1+\sigma_2}{\bar{\sigma}}\} + \frac{3}{4} \frac{\sigma_1-\sigma_2}{\bar{\sigma}}] d\bar{\varepsilon}^p = c_4$
Ayada-m (modified Ayada model)	$\int_0^{\bar{\varepsilon}_f^p} \langle \frac{\sigma_m}{\bar{\sigma}} + \frac{1}{3} \rangle d\bar{\varepsilon}^p = c_5 \langle x \rangle = \{^{x \text{ when } x \geq 0}_{0 \text{ when } x < 0}$
LeRoy et al. (LeRoy)	$\int_0^{\bar{\varepsilon}_f^p} (\sigma_1 - \sigma_m) d\bar{\varepsilon}^p = c_6$

Where $\bar{\varepsilon}_f^p$ is the fracture plastic strain, $\bar{\varepsilon}^p$ is the equivalent plastic strain, σ_1 is the first principal tensile stress, σ_2 is the second principal tensile stress, $\bar{\sigma}$ is the Von Mises equivalent stress, σ_m is the mean (hydrostatic) stress, n is the hardening exponent, c_1–c_6 are the damage limits.

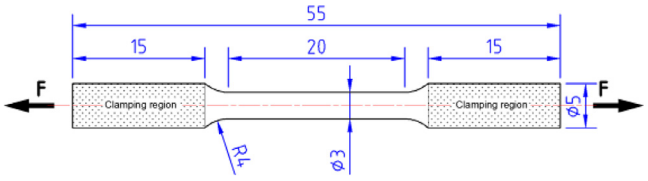

Fig. 1. The sample size for the tensile test.

3. Experiment results

3.1. Tensile test

The tensile tests were conducted using an INSTRON 1186 testing machine with a 100 kN load cell. The geometry of the cylindrical samples was presented in Fig. 1. The sudden drop in the load magnitude during loading was identified as the moment of fracture.

3.2. Experiment of tube spinning

During tube spinning in this study, the tubular blank was clamped against the mandrel by a tailstock and rotated with the mandrel, and the rollers moved parallel to the axial direction on the surface of the tube blank, resulting in uniformly reduced wall thickness and gradually increased length of tubular workpiece, thus the roller feeding trajectory was actually a space spiral line. In the tube spinning experiment, three rollers were distributed uniformly at 120° interval around the mandrel without axial and radial staggered distance. The Ti–15–3 (Ti–15V–3Cr–3Sn–3Al) alloy was used as experimental material for tube spinning. As the Ti–15–3 alloy was a near β titanium alloy with relatively low ductility (the elongation is 10.2%), the cold spinning experiment was conducted within three passes. The tube blanks for spinning experiment were machined from hot forged bars, Φ80 mm in inner diameter, 120 mm in length and 6 mm in thickness. The spinning experiment results are listed in Table 2. According to the experiment result, the thinning rate exhibited obvious influence on the tube spinning process, as shown in Fig. 2. The crack occurred on the inner surface when the thinning rate was smaller at 18.2%, while the crack initiated from the outer surface when the thinning rate was bigger at 42.3%. Only when the moderate thinning rate (27–33%) and solution treatment between